Nuclear Instruments and Methods in Physics Research B 337 (2014) 7–10

Contents lists available at ScienceDirect

Nuclear Instruments and Methods in Physics Research B

journal homepage: www.elsevier.com/locate/nimb

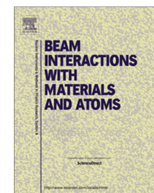

Electrical activation of ion implanted Si in amorphous and crystalline $In_{0.53}Ga_{0.47}As$

A.G. Lind [a,*], M.A. Gill [a], C. Hatem [b], K.S. Jones [a]

[a] Department of Materials Science and Engineering, University of Florida, Gainesville, FL 32611, USA
[b] Applied Materials, Gloucester, MA 01930, USA

A R T I C L E I N F O

Article history:
Received 13 June 2014
Received in revised form 8 July 2014
Accepted 8 July 2014

Keywords:
Ion implantation
Semiconductors
III–V
Amorphization
Activation

A B S T R A C T

The effect of pre-amorphization on the electrical activation of Si implants into $In_{0.53}Ga_{0.47}As$ is investigated. Electrical measurements show that Si implants into pre-amorphized and crystalline $In_{0.53}Ga_{0.47}As$ yield similar levels of activation ($1.0 \times 10^{19}\ cm^{-3}$ in the pre-amorphized case and $9.0 \times 10^{18} cm^{-3}$ in the crystalline case) upon rapid thermal annealing for 5 s at 750 °C despite having very different types of resulting damage in the electrically active layers. The subsequent microstructural characterization by TEM indicates that the highly defective regrown layers in the pre-amorphized substrate leads to poor mobility in the active layers, which result in lower sheet resistances. The results suggest that solid phase epitaxy (SPE) in compound semiconductors can lead to some improved activation at lower temperatures and does not prevent substitutional activation of amphoteric dopants upon post SPE annealing.
© 2014 Elsevier B.V. All rights reserved.

1. Introduction

III–V materials such as $In_xGa_{1-x}As$ and InAs are some of the most promising candidates for future generations of n-channel devices as the electron mobilities of III–V materials are considerably higher than that of Si which has subsequently led to a renewed interest in studying the activation of dopants in III–V materials [1]. For source/drain doping in silicon, high implant doses that are amorphizing at room temperature are often used to achieve the highest activation and most abrupt junctions but the amorphization of cubic III–V semiconductors is generally undesirable as the re-grown layers exhibit high densities of microtwins and stacking faults upon annealing that are stable to high fractions of the respective compounds melting temperature [2–5]. Solid phase epitaxial growth (SPEG) has been shown to be an efficient means of dopant incorporation at reduced temperatures in Si and Ge but studies of dopant activation during solid phase epitaxial growth in III–V materials such as GaAs indicate that III–V materials require annealing temperatures well beyond what is necessary to regrow the amorphous layer to yield activate implanted dopants [6–9]. It is known that avoiding amorphization in III–V's using elevated temperatures results in lower sheet resistances of implanted dopants but it is unclear whether the origin of the more resistive regrown layers is from low solubility of dopants in the regrown layer due to compensation poor incorporation of dopants onto lattice sites during solid phase epitaxial growth (SPEG), or defect related reductions in mobility [10–13]. This study builds on previous works with an in-depth investigation the electrical properties of amorphizing and non-amorphizing implants to determine the origin of increased resistivity in amorphizing implants in Si- doped $In_{0.53}Ga_{0.47}As$. The results of this work indicate that post implantation annealing yields similar donor solubilities in amorphized or crystalline $In_{0.53}Ga_{0.47}As$ for the implant energies and doses studied and that the increase in resistance observed for amorphizing implants is due to large reductions in mobility resulting from highly defective regrown material.

Commercially available (001) InP wafers with 300 nm of lattice matched $In_{0.53}Ga_{0.47}As$ grown by MOCVD were used for this work. A pre-amorphized layer of the $In_{0.53}Ga_{0.47}As$ was achieved with a 220 keV, $3 \times 10^{14}\ cm^{-2}$ As^+ implant performed at room temperature and then Si^+ was subsequently implanted at 20 keV to a fluence of $6 \times 10^{14}\ cm^{-2}$. As^+ was chosen to pre-amorphize the substrate to since it should be electrically inactive as it occupies group V sites and the As^+ energy was chosen such that the Si implant profile is entirely within the amorphous layer. For comparison, non-amorphizing 20 keV Si^+ implants at a dose of $6 \times 10^{14}\ cm^{-2}$ Si^+ were achieved by performing the implantation step at a temperature of 250 °C. After implantation, the pre-amorphized and crystalline samples were coated with a 15 nm thick layer of Al_2O_3 deposited via Atomic Layer Deposition (ALD) to prevent decomposition during subsequent activating anneals. The Si

* Corresponding author.
E-mail address: aglind@ufl.edu (A.G. Lind).

http://dx.doi.org/10.1016/j.nimb.2014.07.009
0168-583X/© 2014 Elsevier B.V. All rights reserved.

implants were then activated by a succession of 5 s rapid thermal anneals (RTA) in argon ambient from 450 to 750 °C in 50 °C increments.

Electrical characterization was performed with Hall effect using the Van der Pauw geometry after each annealing step using pressed on indium contacts placed on un-capped corners of the samples. Structural characterization was performed with cross sectional TEM after ion implantation and after the final anneal at 750 °C to compare the as implanted microstructures with those of the post annealing activation microstructures. Fig. 1a shows a cross-sectional TEM image of the 250 °C, 20 keV 6 × 10^{14} cm^{-2} Si^+ implant into $In_{0.53}Ga_{0.47}As$ in Fig. 1(a) shows that amorphization has been avoided for these implant conditions while Fig. 1(b) indicates that the combination of the 220 keV, 3 × 10^{14} cm^{-2} As^+ and 20 keV 6 × 10^{14} cm^{-2} Si^+ implant was sufficient to amorphize the first 250 nm of the $In_{0.53}Ga_{0.47}As$ layer. SIMS of the implanted Si profile into the pre-amorphized and non-amorphized conditions in Fig. 3 shows that the pre-amorphization results in a more abrupt profile and slightly higher peak concentration as is expected from the reduction in channeling compared to the implanted profile observed for the non-amorphizing case. The TEM micrograph of the pre-amorphized substrate after the ALD Al_2O_3 and 450 °C anneal shown in Fig. 1(c) indicates that a 450 °C 5 s RTA in conjunction with the ALD deposition of Al_2O_3 at 250 °C was sufficient to completely recrystallize the amorphized $In_{0.53}Ga_{0.47}As$. It is apparent from Fig. 1(c) that a high density of stacking faults on the close pack (1 1 1) planes result from SPEG of $In_{0.53}Ga_{0.47}As$ in agreement with other investigators who have shown that III–V arsenide's generally exhibit highly defective regrown layers after low temperature annealing treatments [5,14–16]. Fig 2 (a) and (b) shows cross sectional TEM after the final 750 °C anneal for the 20 keV 6 × 10^{14} cm^{-2} Si^+ implants into the non-amorphized and amorphized substrates. Cross-sectional TEM of studies after annealing for 5 s at 750 °C show that the pre-amorphized substrate still exhibit a highly defective regrown layer as evidenced by the presence of stacking faults while the non amorphizing implant exhibits loop type sub-threshold defects. These loops are usually attributed to excess interstitials resulting from the non-conservative nature of the implant [17]. It can be seen from the comparison of the regrown layer in Fig. 1(c) with the post 750 °C anneal micrographs in Fig 2(b) that some of the regrowth related damage is being annealed out, but the layer remains highly defective after the culmination of annealing treatments performed in this work.

Fig. 4 shows the annealing temperature dependent electrical behavior of the 20 keV 6 × 10^{14} cm^{-2} Si^+ implants into the pre-amorphized and crystalline $In_{0.53}Ga_{0.47}As$ substrates. Annealing temperatures of 450 °C result in a higher level of activation for the pre-amorphized condition than for Si implanted into the crystalline substrate. This suggests that SPE in III–V semiconductors may incorporate some dopant onto lattice sites despite the high level of defects. For annealing temperatures of 500 °C or higher the Si implants into crystalline $In_{0.53}Ga_{0.47}As$ result in higher measured sheet numbers relative to the non-amorphizing case. The

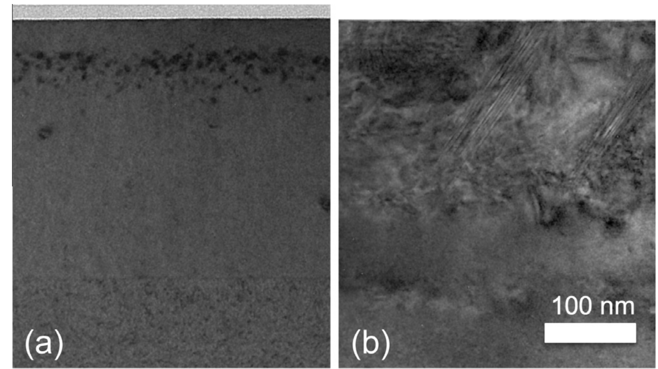

Fig. 2. HR-XTEM images of $In_{0.53}Ga_{0.47}As$ specimens after 750 °C 5 s RTA for (a) 20 keV 6 × 10^{14} cm^{-2} Si^+ implant at 25 °C, (b) 220 keV, 3 × 10^{14} cm^{-2} As^+ and 20 keV 6 × 10^{14} cm^{-2} Si^+ implant at 20 °C.

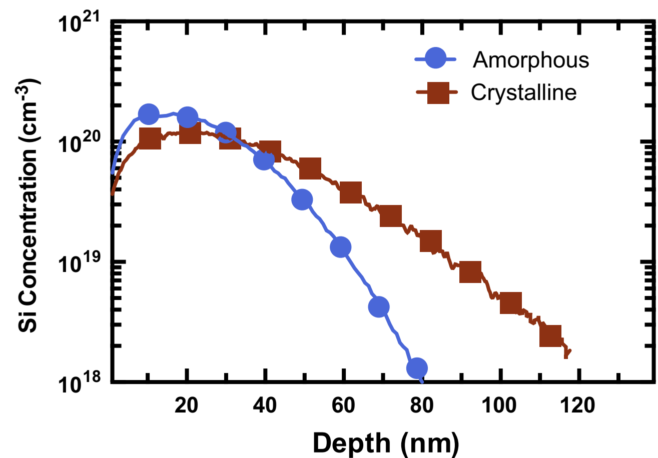

Fig. 3. As-implanted Si concentration profiles for a 20 keV 6 × 10^{14} cm^{-2} Si^+ implant at 20 °C into pre-amorphized $In_{0.53}Ga_{0.47}As$ and at 250 °C into crystalline $In_{0.53}Ga_{0.47}As$.

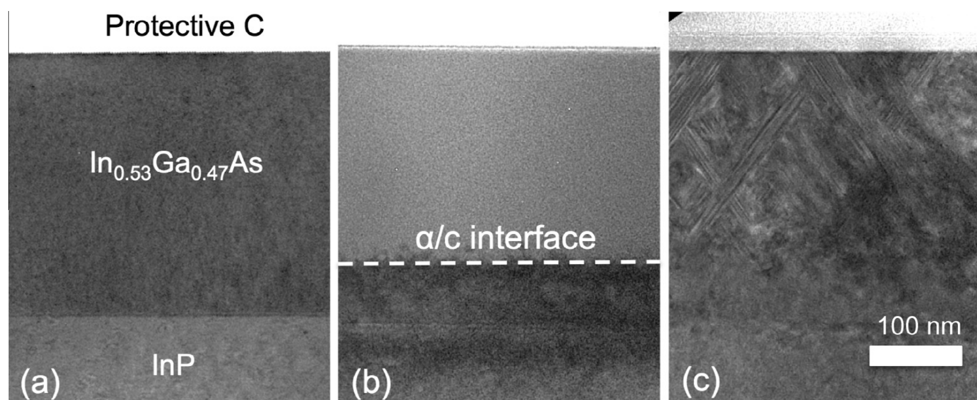

Fig. 1. HR-XTEM images of $In_{0.53}Ga_{0.47}As$ specimens after (a) 20 keV 6 × 10^{14} cm^{-2} Si^+ implant at 25 °C, (b) 220 keV, 3 × 10^{14} cm^{-2} As^+ and 20 keV 6 × 10^{14} cm^{-2} Si^+ implant at 20 °C and (c) 220 keV 3 × 10^{14} cm^{-2} As^+, 20 keV 6 × 10^{14} cm^{-2} Si^+ implant 20 °C after 450 °C 5 s RTA.

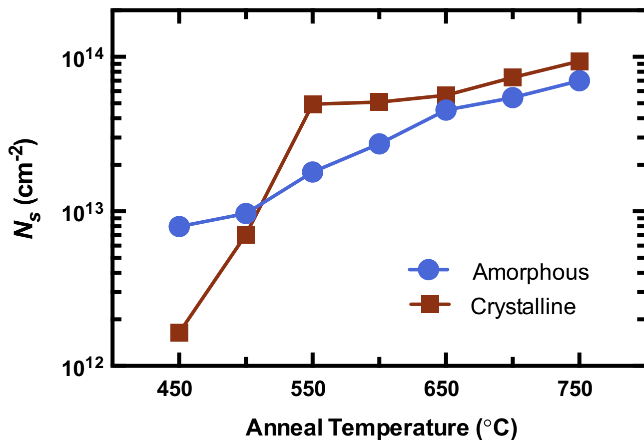

Fig. 4. Active sheet number (N_s) of $In_{0.53}Ga_{0.47}As$ specimens Si^+-implanted at 20 keV to a dose of 6.0×10^{14} cm^{-2} as a function of annealing temperature using a 5 s RTA for Si implants into pre-amorphized and crystalline substrates.

measured sheet number in the pre-amorphized substrate is still very high for anneals of 650–750 °C despite the large amount of damage that remains. This result suggests that the net sheet number of implanted Si in pre-amorphized $In_{0.53}Ga_{0.47}As$, while lower than that of Si implants into crystalline $In_{0.53}Ga_{0.47}As$, is not so severely limited by compensation from damage. The net donor solubility of the two implants was calculated from the as-implanted SIMS profiles in Fig. 3 by assuming negligible diffusion of Si in $In_{0.53}Ga_{0.47}As$ for these annealing temperatures and times. The calculated net donor solubility of Si is 1.0×10^{19} cm^{-3} in the pre-amorphized case and 9.0×10^{18} cm^{-3} in the non-amorphizing case is consistent with previous reports showing Si implants in InGaAs having net donor solubilities in the range of 0.5–1.5 $\times 10^{19}$ cm^{-3} [13,18–20]. Despite the micrographs showing the pre-amorphized substrate being much more defective, the net donor solubility of Si implants in the pre-amorphized substrate is calculated to be slightly higher in the pre-amorphized substrate than the crystalline substrate.

Fig. 5 shows the mobility of the pre-amorphized substrate is significantly reduced in comparison to the crystalline substrate across the entire annealing range studied. The mobility of Si implants into the crystalline materials show an abrupt decrease around 550 °C which is attributed to increased ionized impurity scattering coinciding with the large increase in activation seen at this annealing temperature. The steady improvement in mobility observed for the pre-amorphized substrate indicates that the damage is being annealed out of the regrown layer, but the maximum mobility for the pre-amorphized substrate at 750 °C is only 1/3 of that of the crystalline substrate despite having similar levels of ionized impurities. This suggests that the mobility of the pre-amorphized substrate is severely limited by defects resulting from SPEG and not ionized impurity scattering. Even though the net donor solubility of Si in the pre-amorphized substrate is slightly higher than that in the crystalline substrate, the large reduction in mobility due to the damaged layer results in non-amorphizing implants having consistently lower sheet resistances for all annealing conditions studied as indicated in Fig. 6. The much higher sheet resistances of the pre-amorphized implants potentially limits the practicality of dopant incorporation via SPE unless regrowth related defects are avoided.

Most work aimed at applications of source/drain doping in III–V's has generally sought to avoid amorphization due to the stable nature of damage in III–V materials and reduction in activation that is generally observed. However, studies of Be, Si and Se implants into pre-amorphized GaAs have been performed with vastly different results [21,22]. Be implants into pre-amorphized GaAs have shown higher levels of dopant activation than implants into their crystalline counterparts whereas studies of Si and Se into GaAs that was pre-amorphized by As have shown no n-type activation upon SPE and subsequent annealing suggesting that amorphous layer creation could be an effective way to form electrically inactive layers in n-GaAs [22]. The lack of activation of Si and Se in GaAs that was pre-amorphized was attributed to the precipitation of impurities that formed stacking fault tetrahedras that were visible with HR-TEM. HR-TEM was performed on pre-amorphized Si implants into $In_{0.53}Ga_{0.47}As$ used in this study but no evidence of precipitates was observed despite using much higher doses than were used for the study of Si in GaAs. P-type implant damage is another possible reason for this increase in activation in Be-implanted substrates and negligible activation in Se and Si implants given that previous reports generally indicate that implant damage in III–V arsenides is p-type [23]. However, the results in this paper suggest that at higher Si doses good activation is possible in pre-amorphized $In_{0.53}Ga_{0.47}As$.

In conclusion, Si implanted into pre-amorphized $In_{0.53}Ga_{0.47}As$ has been observed to activate to similar levels as Si implants into crystalline substrates at sufficiently high annealing temperatures for the implant energies and doses studied. The observation of increased Si activation at low temperatures suggests SPEG in

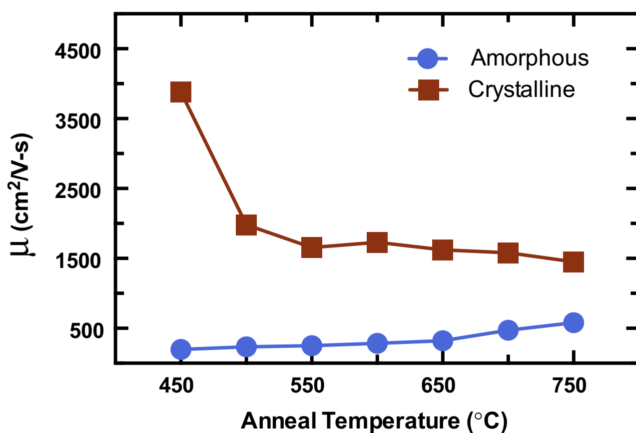

Fig. 5. Mobility (μ) of $In_{0.53}Ga_{0.47}As$ specimens Si^+-implanted at 20 keV to a dose of 6.0×10^{14} cm^{-2} as a function of annealing temperature using a 5 s RTA for Si implants into pre-amorphized and crystalline substrates.

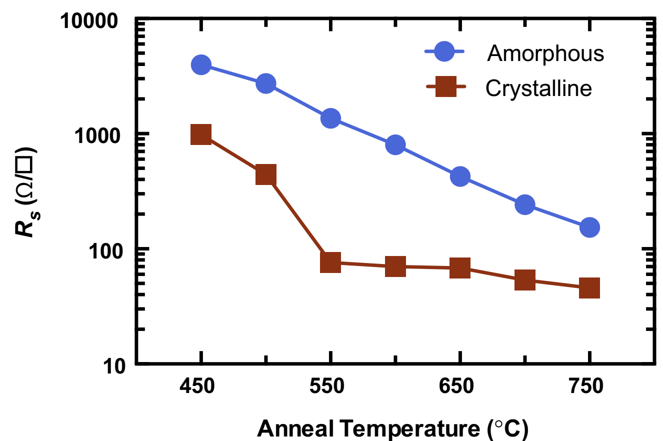

Fig. 6. Sheet resistance (R_s) of $In_{0.53}Ga_{0.47}As$ specimens Si^+-implanted at 20 keV to a dose of 6.0×10^{14} cm^{-2} as a function of annealing temperature using a 5 s RTA for Si implants into pre-amorphized and crystalline substrates.

InGaAs can result in dopant incorporation, but corresponding mobility and sheet resistance measurements combined with structural characterization clearly indicate damage in the regrown layers from pre-amorphization results in higher sheet resistances compared to those of non-amorphizing implants. This result is in sharp contrast to previous work that has shown Si implants into pre-amorphized GaAs to be electrically inactive. Higher annealing temperatures or longer annealing times may result in further activation improvements coming from reductions in residual damage, but the tendency of InGaAs to undergo component evaporation with resultant surface degradation yields a practical limit to damage recovery depending on encapsulation and annealing methods. Pre-amorphization negatively affects the overall sheet resistance, however, as damage in the regrown layer yields greatly reduced mobilities of pre-amorphized substrates compared to those of crystalline substrates. As a result, sheet resistance of pre-amorphized implants is observed to be almost twice that of the sheet resistances measured for implants into crystalline substrates. Lower energy implants resulting in shallower amorphous layers have been shown to exhibit fewer stacking faults [13] suggesting that low energy pre-amorphization combined with low energy Si implants might produce junctions with comparable sheet resistances but more abrupt profiles.

Acknowledgments

The authors acknowledge the Semiconductor Research Corporation for funding this work. The Major Analytical Instrumentation Center at the University of Florida is acknowledged for use of the transmission electron microscopy and focused ion beam facilities.

References

[1] J.A. del Alamo, Nature 479 (2011) 317.
[2] M.A. Shahid, M. Anjum, B.J. Sealy, S.S. Gill, H.J. Marsh, Vacuum 34 (1984) 867.
[3] M. Taniwaki, H. Koide, N. Yoshimoto, T. Yoshiie, S. Ohnuki, M. Maeda, K. Sassa, J. Appl. Phys. 67 (1990) 4036.
[4] R.S. Bhattacharya, A.K. Rai, P.P. Pronoko, J. Narayan, S.C. Ling, S.R. Wilson, J. Phys. Chem. Solids 44 (1983) 61.
[5] C. Licoppe, Y.I. Nissim, C. Meriadec, P. Hénoc, Appl. Phys. Lett. 50 (1987) 1648.
[6] J.S. Williams, Appl. Phys. Lett. 40 (1982) 266.
[7] S.-I. Kwun, C.-H. Hong, W.G. Spitzer, J. Appl. Phys. 54 (1983) 3125.
[8] A. Satta, E. Simoen, T. Clarysse, T. Janssens, A. Benedetti, B. De Jaeger, M. Meuris, W. Vandervorst, Appl. Phys. Lett. 87 (2005) 172109.
[9] H. Nishi, T. Sakurai, T. Furuya, J. Electrochem. Soc. 125 (1978) 461.
[10] S. Pearton, Mater. Sci. Rep. 4 (1990) 313.
[11] D.E. Davies, Appl. Phys. Lett. 23 (1973) 615.
[12] E.V.K. Rao, N. Duhamel, P.N. Favennec, H. L'Haridon, J. Appl. Phys. 49 (1978) 3898.
[13] A.G. Lind, N.G. Rudawski, N.J. Vito, C. Hatem, M.C. Ridgway, R. Hengstebeck, B.R. Yates, K.S. Jones, Appl. Phys. Lett. 103 (2013) 232102.
[14] S.J. Pearton, Int. J. Mod. Phys. B 7 (1993) 4687.
[15] J.S. Williams, M.W. Austin, Appl. Phys. Lett. 36 (1980) 994.
[16] S.M. Hogg, D.J. Llewellyn, H.H. Tan, M.C. Ridgway, Appl. Phys. Lett. 71 (1997) 1397.
[17] K.S. Jones, S. Prussin, E.R. Weber, Appl. Phys. A 45 (1988) 1.
[18] A. Alian, G. Brammertz, N. Waldron, C. Merckling, G. Hellings, H.C. Lin, W.E. Wang, M. Meuris, E. Simoen, K. De Meyer, M. Heyns, Microelectron. Eng. 88 (2011) 155.
[19] M.V. Rao, S.M. Gulwadi, P.E. Thompson, A. Fathimulla, O.A. Aina, J. Electron. Mater. 18 (1989) 131.
[20] A.N.M.M. Choudhury, Appl. Phys. Lett. 40 (1982) 607.
[21] W.G. Opyd, J.F. Gibbons, J. Appl. Phys. 67 (1990) 7417.
[22] W.G. Opyd, J.F. Gibbons, A.J. Mardinly, Appl. Phys. Lett. 53 (1988) 1515.
[23] A.J. Moll, J.W. Ager, K.M. Yu, W. Walukiewicz, E.E. Haller, J. Appl. Phys. 74 (1993) 7118.